Journal of Rehabilitation in Civil Engineering 6-2 (2018) 77-91

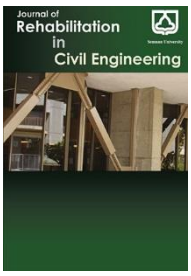

journal homepage: http://civiljournal.semnan.ac.ir/

Soil Structure Interaction Effects on Hysteretic Energy Demand for Stiffness Degrading Systems Built on Flexible Soil Sites

B. Ganjavi [1*], M. Bararnia [2] and A. Azad [3]

1. Assistant Professor, Department of Civil Engineering, University of Mazandaran, Babolsar, Iran
2. PhD Student, Department of Civil, Water & Environmental Engineering, Shahid Beheshti University, Tehran, Iran.
2. Graduate Student, Department of Civil Engineering, University of Mazandaran, Babolsar, Iran

Corresponding author: *b.ganjavi@umz.ac.ir*

ARTICLE INFO

Article history:
Received: 07 July 2017
Accepted: 05 September 2017

Keywords:
Soil-Structure Interaction,
Plastic Energy Demand,
Stiffness Degrading Material,
Cone Models,
Shallow Foundation.

ABSTRACT

This paper aims to investigate the effect of soil-structure interaction on plastic energy demand spectra directly derived from the energy-balance equations of soil-shallow-foundation structure with respect to an ensemble of far-field strong ground motions recorded on alluvium soil. The superstructure is modeled as a single-degree-of-freedom (SDOF) oscillator with Modified Clough stiffness degrading model resting on flexible soil. The soil below the superstructure is modeled as a homogeneous elastic half space and is considered through the concept of Cone shallow foundation Models. A parametric study is carried out for 2400 soil-structure systems with various aspect ratios of the building as well as dimensionless frequency with wide range of fundamental fixed-base period and target ductility demand values subject to an ensemble of 19 earthquakes. Results show that generally for the structure located on softer soils severe dissipated energy drop will be observed with respect to the corresponding fixed-base system. The only exception is for the case of short period slender buildings in which the hysteretic energy demand of soil-structure systems could be up to 70% larger than that of their fixed-base counterparts. Moreover, dissipated energy spectra are much more sensitive to the variation of target ductility especially for the case of drastic SSI effect.

1. Introduction

During the past three decades, remarkable efforts were made to substitute the traditional design strategies by the new method based on the concept of performance-based seismic design. Current seismic analysis methods and design codes are based on strength and displacement capabilities of the structural members, e.g. ASCE/SEI Standard 41-06 (2006), Eurocode 8 (2005), and Turkish Earthquake Code (2007) [1-3]. The general principle of earthquake resistant design methodologies is to investigate the changes

DOI: 10.22075/JRCE.2017.11842.1201

in structural performance during a strong ground motion, which depends on both strength and displacement characteristics of the structure as well as hysteretic behavior of the structural members. Energy inputted to a structure during an earthquake event is regarded as a) hysteretic energy, c) damping energy and c) kinematic energy. [4]. One of the key parameters for evaluating the load reversals effects is the plastic (i.e., hysteretic) energy that ground motions impart to structures [5-11]. The dissipated energy already defined as the area enclosed by hysteretic loop during an earthquake event is related to the damage potential of system [5, 12]. Using the energy concept to evaluate the seismic demands and design of the structural members was initially discussed by Housner (1956) [13]. Since 1980's, the energy principles in the seismic analysis and design procedure of structural members have been investigated by various researchers [12,14-16]. Fajfar and Vidic (1994) introduced the energy spectra to evaluate the structural resistance against earthquake induced effects [7]. Also, several indices for elastic and inelastic systems were proposed for the calculation of the earthquake input energy and dissipation of induced energy [17, 18]. In addition, the relationship between the seismic demand and the structural response based on energy balance principle was investigated by Leelataviwat et al [19]. More recently, several researches have been performed to propose energy-based design approaches and to assess the damage potential of structures [20-22].

It is known for many years that soil-structure interaction (SSI) influences the dynamic behavior of structures [23, 24]. Due to SSI phenomenon, the natural period of the soil-structure systems is larger than the fixed-base structure counterparts. In addition, soil beneath the structure increases damping ratio of the SSI systems due to the inherent and damping [25]. Recently, many researches have gone into the evaluation of the soil-structure interaction effects on the seismic demands of elastic and inelastic response of buildings [26-32]. Recent studies have shown that the soil-structure interaction decreases the response modification factor of both multiple degree-of-freedom (MDOF) and single degree-of-freedom (SDOF) systems [33]. The change in the dynamic behavior of the interacting system has significant influence on both linear and nonlinear response of structures [24, 34]. Soil-structure interaction effects on the dissipated energy and damage sustained by buildings were investigated by Nakhaei and Ghannad [35, 36].

However, the influences of soil-structure interaction on hysteretic energy of stiffness degraded structures during strong ground motion have not been well addressed and further investigation is deemed necessary. Because of the great virtues of speed and cheapness, in almost all studies already carried out by researchers on inelastic behavior of soil-structure systems the inelastic behavior of superstructure was usually modeled by a bilinear force-deformation relationship in which the effect of stiffness degradation on seismic demands was disregarded. The main objective of this paper is to evaluate the effects of soil-structure interaction on hysteretic energy demand of stiffness degraded structures through an intensive paramedic study.

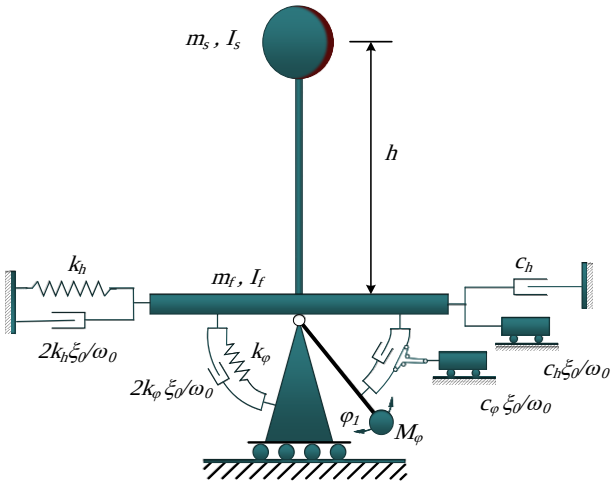

Fig. 1. Soil-shallow foundation structure model used in this study.

2. Soil-Structure Modeling

The soil structure model used in this study to represent the interaction between the superstructure and the underlying soil is shown in Figure 1. As shown in this Figure, the structure is represented by a SDOF oscillator resting on a soil medium. This model is based on the sub-structure method in which the soil and the super-structure are modeled separately and then merged to constitute the soil–structure model. Depicted in Figure 2, the Modified-Clough hysteresis model is used to represent the load-deformation characteristics of superstructure with stiffness degradation. This hysteretic model had been originally proposed by Clough and Johnston [37] and then was modified by Mahin and Bertero [38]. This model has a bilinear envelope, however stiffness degradation after the initial yielding is considered.

The period and viscous damping coefficient of the model are denoted by T and ξ as the fixed-base structure in the first mode of vibration.

For the stance that the structure is viewed as a representative of more complex multistory buildings, the lumped mass, m_s, and the height, h, are the effective mass and the effective height corresponding to the first mode of vibration of the fixed-base structure, respectively. Also, mass moment of inertia, I_s, of the SDOF oscillator is calculated as, $m_s r^2/4$ where r is the equivalent circular floor's radius. In addition, the foundation is modeled as a circular rigid disk with no embedment lying on the surface of the soil with mass m_f and mass moment of inertia I_f. Similar to I_s, I_f can be computed as $m_f r^2/4$. Because the rigid surface foundation is subjected to vertically incident plane shear waves, only inertial part of the soil-structure interaction is considered and the kinematic interaction can be ignored.

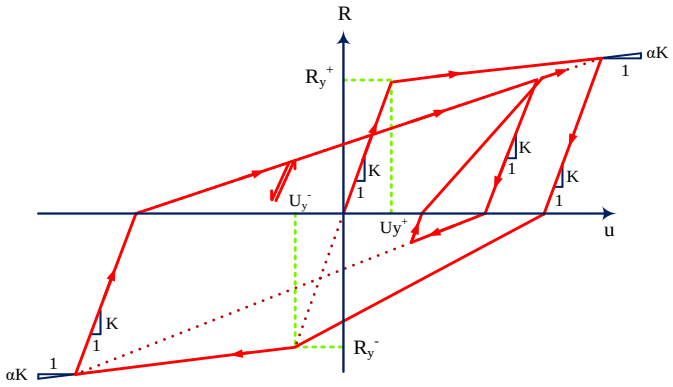

Fig. 2. Modified Clough Bilinear Stiffness Degrading Model.

The soil is modeled as a homogenous half-space medium through an equivalent linear discrete model based on the concept of truncated cone model [39]. Cone model is based on the one dimensional wave propagation theory, which frequently utilized to simulate SSI with adequate precision in practice [40]. The soil below the structure is substituted with a three-DOF dashpot and spring system. Two DOFs are defined for the horizontal (sway) and the rocking, φ, that are introduced as the representatives of the and the rotational and translational movements of the foundation, respectively, neglecting the minor influences of vertical and torsional movements of the foundation. The third one as an internal DOF, φ_1, is introduced in the soil model that allows the frequency dependency of the rotational spring and dashpot coefficients to be taken into account. This additional internal rotational DOF, is augmented to a polar mass moment of inertia, M_φ, placed in series with the rotational dashpot.

The dashpots and springs' coefficients for translational and rocking motions are defined as [39]:

$$K_h = \frac{8\rho V_s^{\,2} r}{2-\nu}, \qquad c_h = \pi \rho V_s r^2, \quad (1)$$

$$K_\varphi = \frac{8\rho V_s^{\,2} r^3}{3(1-\nu)}, \qquad c_\varphi = \frac{\pi}{4}\rho V_p r^4, \quad (2)$$

$$M_\varphi = \frac{9\rho\pi^2 r^5 (1-\nu)}{32}\left(\frac{V_p}{V_s}\right)^2 \quad (3)$$

in which K_h, c_h, K_φ, and c_φ are the translational stiffness, translational viscous damping, rocking stiffness and rocking viscous damping, respectively. Besides, r, ρ, ν, V_p and V_s are the equivalent circular foundation' radius, specific mass, poisson's ratio, and the primary and secondary (shear) wave velocities of soil, respectively. Also, a trapped mass moment of inertia ΔM_φ equal to $0.3\pi(\upsilon - 1/3)\rho r^5$, which modifies the effect of soil incompressibility, is assigned to the foundation nod. In this regards, ΔM_φ is added to I_f ν larger than 1/3[39].

3. Key Interacting Parameters

Under an earthquake event, the response of the SSI system depends basically on the structural and soil features. In other words, the dynamic response of the structure under a given earthquake excitation can be interpreted based on the the structural size, its vibration and soil characteristics as well as

the induced excitation. It has been shown that the main features of soil-structure systems can be adequately defined by the following dimensionless key parameters [24, 41].

(1) A dimensionless frequency is expressed as a representative of the ratio of the structure to soil stiffness:

$$a_0 = \frac{\omega_n h}{V_s} \quad (4)$$

where ω_n, h and V_s are the circular frequency of the system without SSI effect, the effective structural height and velocity of S wave, respectively. It is worth mentioning that the applicable range of this parameter for requlars building structures is between 0, for the FB structure and up to 3, for the case with predominant soil-structure interaction effect.

(2) The slenderness ratio of the structure is described as the structural height to foundation radius ratio, h/r, which is an index for its slenderness ratio.

(3) Inepter-story ductility demand for a structure defined as:

$$\mu = \frac{u_m}{u_y} \quad (5)$$

Where u_y and u_m are the yield displacement and the maximum displacement due to specific ground motion, respectively.

(4) The ratio of structure to soil mass index defined as:

$$\bar{m} = \frac{m}{\rho r^2 h} \quad (6)$$

(5) The ratio of foundation to structural mass m_f/m_s.

(6) Poisson ratio of soil ν.

(7) Damping ratios of the soil ξ_0 and of the structure ξ.

In this study, the first two factors are used as the key parameters of the soil-structure system that define the main soil-structure interaction effects. The third parameter varies between 2 and 6 with steps of 1, representing low to high levels of non-linearity in the superstructure. The other parameters, having a narrow range of variation for conventional buildings and, hence, depending on a given case they may be set to typical constant values. The assumed values of these parameters are summarized in Table 1.

Table 1. The values of the key design parameters used in this paper.

Design parameter	values
(a_0)	0, 1, 2, 3
(h/r)	1, 3, 5
(μ)	2, 3, 4, 5, 6
$(\bar{m})$	0.5
(m_f/m_s)	0.1
(ν)	0.4
Damping ratios of the soil (ξ_0) and of the structure (ξ)	0.05

4. Equation of Motion and Hysteretic Energy

For an *n* DOFs inelastic system the equation of motion of under a horizontal earthquake acclamation, depicted in Fig. 1 can be defined as

$$\mathbf{M}\ddot{u}(t)+\mathbf{C}\dot{u}(t)+F_s(u,\dot{u})=-\mathbf{M}r\ddot{u}_g(t) \quad (7)$$

In which **M** is the mass matrix of structure, **C** is the viscous damping coefficient matrix, $\ddot{u}_g$ is the base acceleration, $F_s(t)$ = the hysteretic restoring force vector corresponding to nonlinear force-deformation relationship of the system (Figure 2), r = an dimensionless influence vector and $u,\dot{u},\ddot{u}$ are respectively the relative displacement, velocity and acceleration vector of the mass.

Integrating the differential equation of motion i.e., Equation (7) with respect to u leads to the following equation which must be valid for entire duration of the ground motion:

$$E_k(t)+E_D(t)+E_H(t)+E_s(t)=E_I(t) \quad (8)$$

The parameter in the right side of Eq. (8) is the input energy which represents the input energy that imparted to the system by the moving base:

$$E_I=-\int_0^t \mathbf{M}r\ddot{u}_g(t)\dot{u}\,dt \quad (9)$$

The first parameter on the left part of Eq. 8 is the mass kinetic energy corresponding to its relative motion with respect to the ground:

$$E_k=\int_0^t \mathbf{M}\ddot{u}(t)\dot{u}(t)\,dt \quad (10)$$

The second parameter on the left part of Eq. 8 is the dissipated energy via viscous damping:

$$E_D=\int_0^t \mathbf{C}\dot{u}^2(t)dt \quad (11)$$

The last terms on the left side of Eq.8 are the dissipated energy through plastic behavior (E_Y) and the elastic strain energy (E_s) of the system:

$$E_Y+E_s=\int_0^t F_s(t)\dot{u}(t)dt \quad (12)$$

Based on Eq. 12, dissipated hysteresis energy (E_Y) is computed for each soil-structure system under a given earthquake records.

5. Selected Earthquake Ground Motions

In this paper a family of nineteen acceleration time history records have been compiled from PEER. The utilized ground motions are classified by NEHRP as site class D [18]. They have been recorded during 9 earthquake events with magnitude varying from 6.6 to 7.7 at distance between 10 and 28 Km.

The utulized accelerations have the properties including: (i) they have magnitude larger than 6.5; (ii) Distance from earthquake source to structures location more than 10 Km; (iii) One of the two horizontal components has a (PGA) and (PGV) larger than 0.2g and 15 cm/sec, respectively; (iv) they are not classified as pulse type record in the PEER database. The main characteristics of the selected ground motions are listed in **Error! Reference source not found.**. For each event, the horizontal component with

greater PGV is considered as the "strong" acceleration and the other record is selected as the "weak" one. In this paper, results are reported based on the strong accelerations.

The response of elastic spectra of strong accelerations along their average values are shown in Fig. 3.

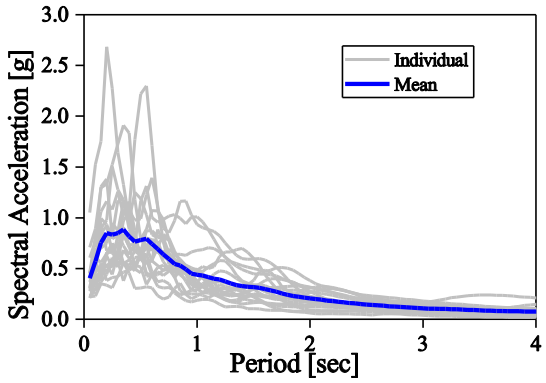

Fig. 3. The response of elastic spectra of strong accelerations along their average values**.**

6. Method of Analysis

The Four DOF SSI model described in this paper has the sufficiency to be codified in time domain directly. In this regard, a comprehensive SSI analysis program is written and developed using MATLAB using β-Newmark's method with modified Newton-Raphson technique. An intensive parametric study is conducted using a family of 2400 SSI systems including 4 dimensionless key parameters,(a_0 = 0, 1, 2, 3), three values of aspect ratio (h/r =1, 3, 5), five values of target drift ductility (μ = 2, 3, 4, 5, 6) and wide range of fixed-base fundamental period of vibration ranging from 0.1s to 5 s (varied from 0.1s to 1 s, with 0.05 s steps, 1.1s to 3 with 0.1s steps and 3.2 s to 5 s with 0.2 s steps) subjected to 19 earthquake ground motions.

For a given fixed-based period, in the first step, the structural yield strength is computed by using an iterative algorithm proposed by Ganjavi and Hao (2012, 2014) To reach the obtain the target ductility within 0.5% of accuracy when undergone to a given acceleration [33]. The plastic hysteretic energy normalized to total mass in the structure is then computed accordingly. The influence of Soil-Structure-Interaction on hysteretic energy demand spectra can be examined by comparing the spectra for predefined cases. Note that SSI systems with a_0 = 0 are indeed associated with the fixed-base system, whereas a_0 = 2 and 3 can be considered as the representatives of systems with predominant SSI effect.

Table 2. List of earthquakes ground motions recorded on site class D of NEHRP based on V_s.

Station Name	Event*	Mag.	Year	ClstD [km]	Strong			Weak		
					A_g [g]	V_g [cm/s]	D_g [cm]	A_g [g]	V_g [cm/s]	D_g [cm]
LA - Hollywood Stor FF	1	6.61	1971	22.8	0.2	21.7	15.9	0.2	16.9	12.9
Calexico Fire Station	2	6.53	1979	10.5	0.3	22.5	9.9	0.2	18.7	15.9
Delta	2	6.53	1979	22.0	0.3	33.0	20.2	0.2	26.3	14.7
El Centro Array #11	2	6.53	1979	12.6	0.4	44.6	21.3	0.4	36.0	25.1
El Centro Imp. Co. Cent	3	6.54	1987	18.2	0.4	48.1	19.3	0.3	41.8	21.9

Westmorland Fire Sta	3	6.54	1987	13.0	0.2	32.3	22.3	0.2	23.5	15.0
Capitola	4	6.93	1989	15.2	0.5	38.0	7.1	0.4	29.6	4.9
Hollister - South & Pine	4	6.93	1989	27.9	0.4	63.0	32.3	0.2	30.9	19.7
Hollister City Hall	4	6.93	1989	27.6	0.2	45.5	28.5	0.2	38.9	19.4
Hollister Differential Array	4	6.93	1989	24.8	0.3	44.2	19.7	0.3	35.8	14.6
Beverly Hills – 14145 Mulhol	5	6.69	1994	17.2	0.5	66.7	12.2	0.4	59.3	15.5
Canyon Country - W Lost Cany	5	6.69	1994	12.4	0.4	44.4	11.3	0.5	41.1	14.6
LA - Saturn St	5	6.69	1994	27.0	0.4	41.6	5.0	0.5	37.2	4.4
Santa Monica City Hall	5	6.69	1994	26.5	0.9	41.6	15.2	0.4	25.0	7.4
Kakogawa	6	6.90	1995	22.5	0.3	26.9	8.8	0.2	20.8	6.4
Shin-Osaka	6	6.90	1995	19.2	0.2	31.3	8.4	0.2	21.8	9.7
Duzce	7	7.51	1999	15.4	0.3	58.9	44.1	0.4	55.7	25.0
CHY036	8	7.62	1999	16.0	0.2	44.8	34.0	0.3	41.7	19.5
Fortuna Fire Station	9	7.01	1992	20.4	0.3	38.1	16.7	0.3	33.9	20.9

* (1) San Fernando; (2) Imperial Valley-06; (3) Superstition Hills-02; (4) Loma Prieta; (5) Northridge-01; (6) Kobe, Japan; (7) Kocaeli, Turkey; (8) Chi-Chi, Taiwan; (9) Cape Mendocino

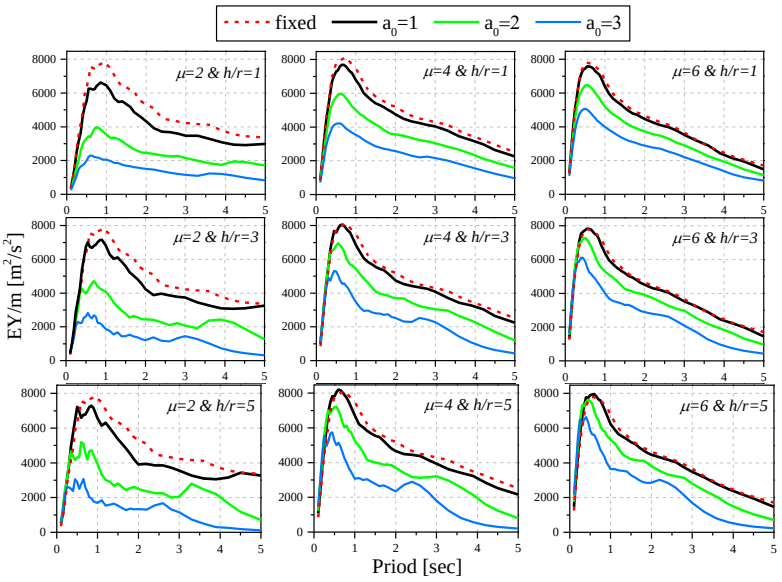

Fig. 4. Effect of structure-to soil stiffness ration on hysteretic energy demand.

7. Results and Discussion

7.1. Effect of Foundation Flexibility

To examine the effect of soil stiffness on hysteretic energy demand spectra of soil-structure systems Figure 4 is depicted. In each of the graphs presented in this part, the a_0 value is varied under constant target ductility μ and constant aspect ratio *h/r*. The results are for the average values of E_Y/m from 19 records for soil-structure systems with *h/r* = 1, 3, 5, three ductility ratios (μ= 2, 4, 6), three dimensionless frequencies (a_0 = 1, 2, 3), as well as for the corresponding fixed-base structures. Seemingly, for the location

with softer soils, more considerable interaction between the structure and the soil would be supposed. Albeit, it is worth noting that the governing parameter in the SSI system is the ration of structure to soil stiffness (a_0) and not only that of the soil. As seen, as target ductility demand increases, the differences between the hysteretic energy demand of soil-structures systems and those of the fixed-base ones becomes lower. The graphs show that unlike to the soil-structure systems, energy dissipated in fixed-base systems is not very sensitive to the structural inelastic behavior, i.e., target ductility demand. While for fixed-base systems the peak values of mean hysteretic energy demand normalized to the total mass for different target ductility demands are around 8000 (m^2/s^2) , they, in SSI systems, generally amplifies as target ductility demand increases, which is more pronounced for the case of looser soil (a_0=3). Despite the fact that, the ordinates corresponding to the lower SSI effect i.e., a_0= 1 are nearly the same as the fixed-base one, for greater amounts of dimensionless frequency (a_0= 2, 3), severe energy drop will be observed.

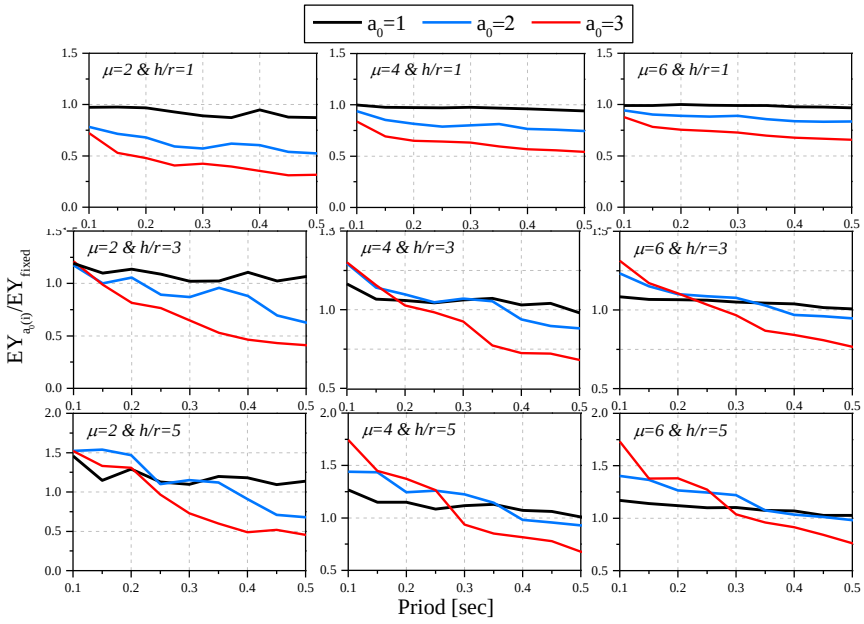

Fig. 5. Effect of structure-to soil stiffness ration on mean hysteretic energy demand spectra in constant acceleration region.

Results show that, except for short period slender buildings, SSI generally reduces the hysteretic energy demand of structures. For better comparison, the ratio of hysteretic energy demand in soil-structure systems to that of the corresponding fixed-base ones are plotted in Figures 5 and 6 for respectively acceleration sensitive region (period less than 0.5 sec) and velocity region (period between 0.5 and 5 sec) for different values of non-dimensional frequency, aspect ratio and target ductility demand. As seen from these

Figures, in squat buildings (h/r = 1) for both acceleration and velocity regions, less energy is dissipated through the inelastic behavior of structures as soil becomes looser. However, this trend will not be observed for short period slender buildings (h/r = 3, 5) in constant acceleration region. In fact, in constant acceleration region depending on the value of aspect ratio, there is a threshold period before which the flexible-base hysteretic energy is greater than that of the fixed-base one; afterwards, this trend is reversed. The more the value of h/r, the greater is the difference between hysteretic energies of the flexible-base and the fixed-base systems. In this case, for very short period the hysteretic energy demand of SSI systems could be up to 70% larger than that of their fixed-base counterparts.

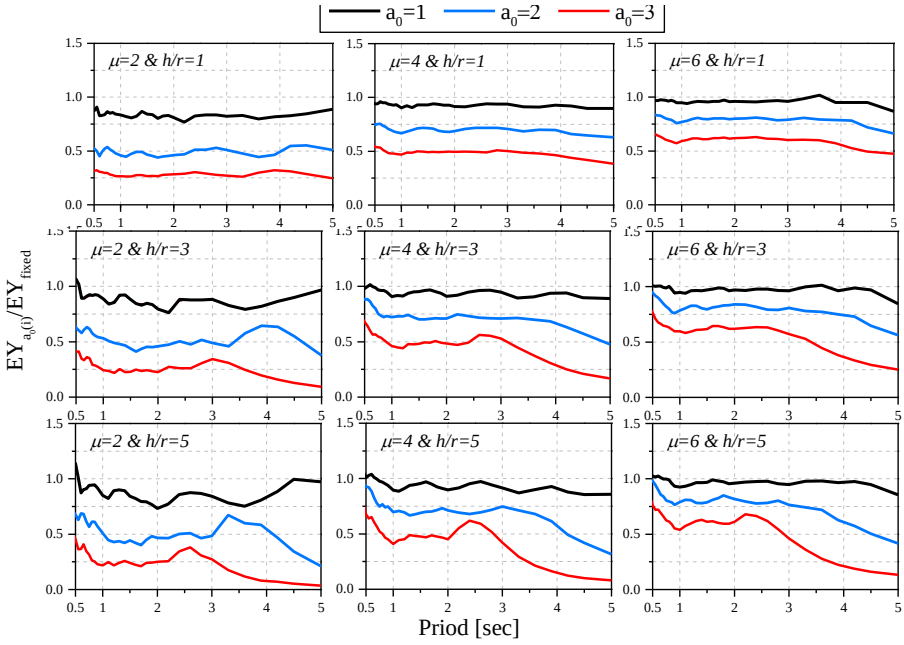

Fig. 6. Effect of structure-to soil stiffness ration on mean hysteretic energy demand spectra in constant velocity region.

The value of the so-called threshold period increases by increasing the aspect ratio and target ductility demand. With regard to the substantial growth in the ductility demands of such structures under sever SSI effect; this amplification of dissipated energy demand through yielding behavior is justified (Ganjavi et al., 2016 [42]; Nakhaei and Ghannad 2006 [36]). Nevertheless, as the slender structures usually have periods larger than the observed threshold period, it may deduce that normally SSI diminishes the hysteretic demands of structures. Nearly the same conclusion was reported by Nakhaei and Ghannad 2006 for bilinear non-deteriorating elastic-plastic hysteretic behavior though unlike to the present study, in their research [42] the yield strength of the SSI systems was considered as the yield strength of the corresponding fixed-base building for the prespecified target ductility due to a given earthquake acceleration.

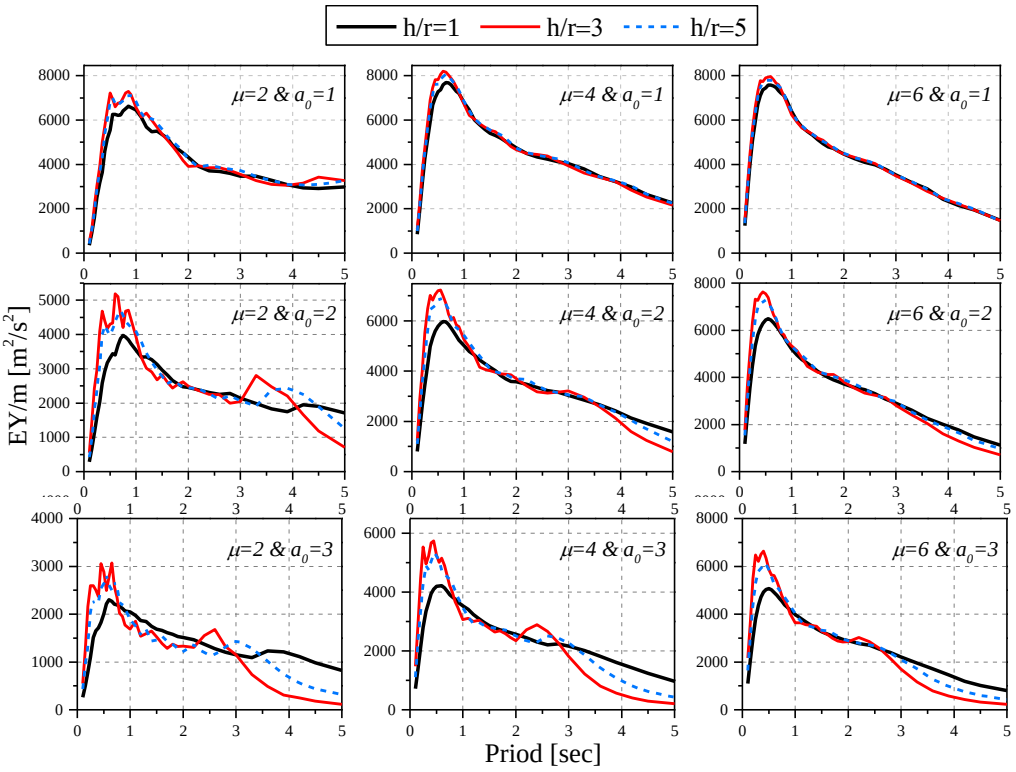

Fig. 7. Effect of Building aspect ratio on mean hysteretic energy demand spectra.

7.2. Effect of Building Aspect Ratio

In this section the influence of the slenderness ratio of the superstructure on the hysteretic energy demand spectra of the SSI system is examined as illustrated in Figure 7. The results are provided as mean dissipated energy demand for different soil-structure systems in both aforementioned period regions. In this graph, on contrary to the previous section, the aspect ratio is varied by the values of 1, 3 and 5 representing squat, average and slender building, respectively, while the two other key parameters i.e., the (a_0) and (μ) remain constant. In this figure the hysteretic energy demand for the cases of fixed-base systems are not shown since the aspect ratio has nothing to do with these systems. It can be observed that for the systems with insignificant SSI effect (i.e. a_0 =1), except for the low level of target ductility demand, intensifying the *h/r* will not significantly change the mean hysteretic energy demand values. However, by increasing the a_0, the effect of slenderness ratio ,*h/r*, on SSI systems would be more pronounced. In soil-structure systems with more drastic SSI effect (i.e. a_0 = 2, 3), increasing the slenderness ratio ,*h/r*, is accompanied by increasing the dissipated energy for shorter period and decreasing them for the longer period after a periodic range variable with the ductility demand and non-dimensional frequency values. The phenomenon is more pronounced as the target ductility demand decreases. Again, it is demonstrated that the increase in dissipated energy under the effect of slenderizing will become more noticeable for slender buildings

(i.e., larger *h/r*) with greater a_0 value (i.e. on softer soil profiles).

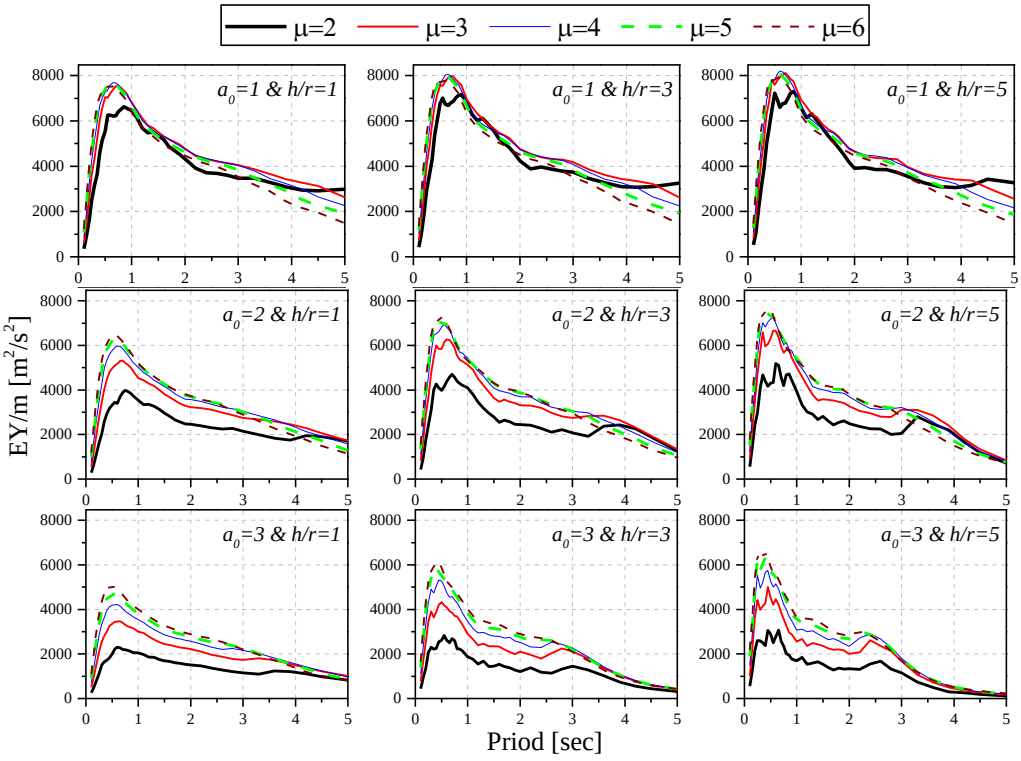

Fig. 8. Effect of target ductility on mean hysteretic energy demand spectra.

7.3. Effect of Target Ductility on Hysteretic Energy Demand

Similar to the trend that was considered in the two previous sections, here, to study the influence of target ductility ratio on dissipated energy demand spectra of SSI systems the μ value is varied while both interaction governing parameters including dimensionless frequency a_0 and aspect ratio *h/r* are constant. The results are for the average values of E_Y/m from 19 earthquake accelerations for soil-structure systems with *h/r* = 1, 3, 5, three dimensionless frequencies (a_0 = 1, 2, 3) having five target ductility ratios (μ= 2, 3, 4, 5, 6) as shown in Figure 8.

The results can be classified as two parts; (1) In slight SSI effect with the structure-to-soil stiffness ratio (a_0 = 1) irrespective of the value of *h/r* , except for the very low level of ductility demand equal to 2, peak values of dissipated energy are not sensitive to the variation of the ductility demand. Nevertheless, as the structural period increases the values of hysteric energy demand conversely decreases with increasing the target ductility. (2) For the case of nearly moderate (a_0 = 2) and drastic SSI effect (a_0 = 3) the trend is different in such a way that, except for very short and very long periods, the more the target ductility demand, the greater is the dissipated energy demand, which is more pronounced for the case of softer soil with non-dimensional frequency equal to 3. Nonetheless, it should also be noted that dissipated energy demand is less sensitive to the variation of the target ductility for high level of inelastic behavior (i.e., μ > 4). Moreover, for this case the

differences between dissipated energy demands correspond to the different ductility demands usually become negligible towards longer periods (i.e., larger than 4 s). The trend is roughly similar for all values of aspect ratio.

8. Concluding Remark

The primary objectives of the investigations conducted in this paper were to augment our understanding of the importance of soil-structure interaction on plastic energy dissipation of stiffness degrading SDOF soil-shallow-foundation systems through an intensive parametric study. A series of 2400 4-DOFs soil-shallow-foundation structure models were developed based on cone model and analyzed under a family of 19 strong ground motions recorded on alluvium site. The mean plastic energy demand spectra of various fixed-base and flexible-base systems were computed for acceleration and velocity sensitive regions which cover most of common building structures. The primary findings of this study indicate that, except for short period slender buildings, SSI generally reduces the hysteretic energy demand of structures. For constant acceleration region depending on the value of aspect ratio, there is a outset period of vibration before that the flexible-base hysteretic energy is larger than that of the fixed-base hysteretic energy; subsequently, the condition is conversed. The larger the value of aspect ratio, the larger is the difference between hysteretic energies of the flexible-base and the fixed-base systems. In this case, for a very short period the hysteretic energy demand of SSI systems could be up to 70% larger than that of their fixed-base counterparts. Nonetheless, as it is obvious that slender structures practically do not have periods lower than the observed threshold period, it can be deduced that , in general, SSI reduces the hysteretic demands of structures. Moreover, unlike to the fixed-base and slight SSI systems, except for very short and very long periods the dissipated energy spectra are much more sensitive to the variation of target ductility especially for drastic SSI effect. In this case the differences between dissipated energy demands correspond to the different ductility demands usually become negligible towards longer periods (i.e., larger than 4 s). Further researches are required to study the effect of SSI on other energy demand parameters such as input energy, damping energy and the ratio of dissipated to input energy.

REFERENCES

[1] ASCE/SEI (2006). Standard 41-06 Seismic Rehabilitation of Existing Buildings. American Society of Civil Engineers, Reston, Virginia, USA.

[2] urocode 8: (2005). Design of structures for earthquake resistance.

[3] Code TE. (2007). Specification for structures to be built in disaster areas, *Ministry of Public Works and Settlement Government of Republic of Turkey*.

[4] Park Y-J, Ang A-S, Wen Y-K. (1984). Seismic damage analysis and damage-limiting design of RC buildings. University of Illinois Engineering Experiment Station. College of Engineering. University of Illinois at Urbana-Champaign.,

[5] Park Y-J, Ang AH-S. (1985). Mechanistic seismic damage model for reinforced concrete, *Journal of structural engineering*, 111 722-39.

[6] Fajfar P. (1992). Equivalent ductility factors, taking into account low-cycle fatigue, *Earthquake Engineering & Structural Dynamics*, 21 837-48.

[7] Fajfar P, Vidic T. (1994). Consistent inelastic design spectra: hysteretic and input energy,

Earthquake Engineering & Structural Dynamics, 23 523-37.

[8] Rodriguez M. (1994). A measure of the capacity of earthquake ground motions to damage structures, *Earthquake engineering & structural dynamics*, 23 627-43.

[9] Teran-Gilmore A. (1996). Performance-based earthquake-resistant design of framed buildings using energy concepts: University of California, Berkeley;

[10] Manfredi G. (2001). Evaluation of seismic energy demand, *Earthquake Engineering & Structural Dynamics*, 30 485-99.

[11] Riddell R, Garcia J. (2002). Hysteretic energy spectrum and earthquake damage, *7th US NCEE (Boston)*.

[12] Kuwamura H, Galambos TV. (1989). Earthquake load for structural reliability, *Journal of Structural Engineering*, 115 1446-62.

[13] Housner GW, (1959). editor Behavior of structures during earthquakes. Selected Earthquake Engineering Papers of George W Housner: ASCE.

[14] Zahrah TF, Hall WJ. (1984). Earthquake energy absorption in SDOF structures, *Journal of structural Engineering*, 110 1757-72.

[15] Akiyama H. (1985). Earthquake-resistant limit-state design for buildings: Univ of Tokyo Pr.

[16] Bertero V, Uang C. (1988). Implications of recorded earthquake ground motions on seismic design of building structures. Research Report (UCB/EERC-88/13).

[17] Decanini LD, Mollaioli F. (1998). Formulation of elastic earthquake input energy spectra, *Earthquake engineering & structural dynamics*, 27 1503-22.

[18] Decanini LD, Mollaioli F. (2001). An energy-based methodology for the assessment of seismic demand, *Soil Dynamics and Earthquake Engineering*, 21 113-37.

[19] Leelataviwat S, Saewon W, Goel SC. (2009). Application of energy balance concept in seismic evaluation of structures, *Journal of structural engineering*, 135 113-21.

[20] Dindar AA, Yalçin C, Yüksel E, Özkaynak H, Büyüköztürk O. (2015). Development of Earthquake Energy Demand Spectra, *Earthquake Spectra*, 31 1667-89.

[21] Benavent-Climent A, López-Almansa F, Bravo-González DA. (2010). Design energy input spectra for moderate-to-high seismicity regions based on Colombian earthquakes, *Soil dynamics and earthquake engineering*, 30 1129-48.

[22] Sadeghi K. (2011). Energy based structural damage index based on nonlinear numerical simulation of structures subjected to oriented lateral cyclic loading, *International Journal of Civil Engineering*, 9 155-64.

[23] Chopra AK, Gutierrez JA. (1974). Earthquake response analysis of multistorey buildings including foundation interaction, *Earthquake Engineering & Structural Dynamics*, 3 65-77.

[24] Veletsos AS. (1977). Dynamics of structure-foundation systems, *Structural and geotechnical mechanics*, 333-61.

[25] Wolf JP. (1985). Dynamic soil-structure interaction: Prentice Hall int.

[26] Ghannad M, Jahankhah H. (2007). Site-dependent strength reduction factors for soil-structure systems, *Soil Dynamics and Earthquake Engineering*, 27 99-110.

[27] Ganjavi B, Hao H. (2012). A parametric study on the evaluation of ductility demand distribution in multi-degree-of-freedom systems considering soil–structure interaction effects, *Engineering Structures*, 43 88-104.

[28] Tang Y, Zhang J. (2011). Probabilistic seismic demand analysis of a slender RC shear wall considering soil–structure interaction effects, *Engineering Structures*, 33 218-29.

[29] Raychowdhury P. (2011). Seismic response of low-rise steel moment-resisting frame (SMRF) buildings incorporating nonlinear

soil–structure interaction (SSI), *Engineering Structures*, 33 958-67.

[30] Aviles J, Pérez-Rocha LE. (2011). Use of global ductility for design of structure–foundation systems, *Soil Dynamics and Earthquake Engineering*, 31 1018-26.

[31] Khoshnoudian F, Ahmadi E. (2013). Effects of pulse period of near-field ground motions on the seismic demands of soil–MDOF structure systems using mathematical pulse models, *Earthquake Engineering & Structural Dynamics*, 42 1565-82.

[32] Ganjavi B, Hajirasouliha I, Bolourchi A. (2016). Optimum lateral load distribution for seismic design of nonlinear shear-buildings considering soil-structure interaction, *Soil Dynamics and Earthquake Engineering*, 88 356-68.

[33] Ganjavi B, Hao H. (2014). Strength reduction factor for MDOF soil–structure systems, *The Structural Design of Tall and Special Buildings*, 23 161-80.

[34] Bielak J. (1978). Dynamic response of non-linear building-foundation systems, *Earthquake Engineering & Structural Dynamics*, 6 17-30.

[35] Nakhaei M, Ghannad MA. (2008). The effect of soil–structure interaction on damage index of buildings, *Engineering Structures*, 30 1491-9.

[36] Nakhaei M, Ghannad M. (2006). The effect of soil-structure interaction on hysteretic energy demand of buildings, *Structural Engineering and Mechanics*, 24 641-5.

[37] Clough RW. (1966). Effect of stiffness degradation on earthquake ductility requirements: Structural Engineering Laboratory, University of California,

[38] Mahin SA, Bertero VV. (1976). Nonlinear seismic response of a coupled wall system, *Journal of the Structural Division*, 102 1759-80.

[39] Wolf JP. (1994). Foundation vibration analysis using simple physical models: Pearson Education.

[40] Meek JW, Wolf JP. (1993). Why cone models can represent the elastic half-space, *Earthquake engineering & structural dynamics*, 22 759-71.

[41] GHANNAD MA, 福和伸夫, 西阪理永. 11(1998). A STUDY ON THE FREQUENCY AND DAMPING OF SOIL-STRUCTURE SYSTEMS USING A SIMPLIFIED MODEL, *構造工学論文集 B*, 44 85-93.

[42] Ganjavi B, Hao H, Hajirasouliha I. (2016). Influence of Higher Modes on Strength and Ductility Demands of Soil–Structure Systems, *Journal of Earthquake and Tsunami*, 1650006.